

Original Article

Long non-coding RNA H19 protects PC-12 cells from hydrogen peroxide-induced injury by targeting miR-155 in spinal cord injury

Ran Li¹, Fei Yin¹, Yingying Guo², Kunchi Zhao¹, Qing Ruan¹, Yingmei Qi¹

¹Department of Orthopedics, China-Japan Union Hospital of Jilin University, Changchun, P. R. China; ²Department of Blood Transfusion, The First Bethune Hospital of Jilin University, Changchun, P. R. China

Received March 2, 2017; Accepted April 26, 2017; Epub June 1, 2017; Published June 15, 2017

Abstract: Background: Spinal cord injury (SCI) is a serious neurological disease, in which reactive oxygen species, such as hydrogen peroxide (H₂O₂), are produced in excess, causing growth arrest and cell death. The present study evaluated the effects of long non-coding RNA (lncRNA) H19 on H₂O₂-injured pheochromocytoma (PC-12) cells. Methods: H₂O₂ was used to induce injury in PC-12 cells. We then measured the effects of suppression of H19, downregulation of microRNA (miR)-155, and overexpression of forkhead box protein O1 (FOXO1) on viability, migration, invasion, and apoptosis in H₂O₂-injured PC-12 cells in separate experiments. In these experiments, qRT-PCR was used to measure expression levels of different mRNAs and western blot analysis was used to measure different protein expressions. Results: H₂O₂ injured PC-12 cells by decreasing cell viability, migration, and invasion, and increasing apoptosis. Suppression of H19 expression further increased H₂O₂-induced injury in PC-12 cells. Suppression of H19 also increased miR-155 expression, which was identified as a target of H19 using luciferase reporter assay. Downregulation of miR-155 protected PC-12 cells from H₂O₂-induced injury. FOXO1 was identified as a target of miR-155, and expression of FOXO1 was decreased by miR-155 overexpression. RT-PCR and western blot analysis revealed that overexpression of FOXO1 decreased H₂O₂-induced PC-12 cell injury by activating PI3K/AKT and Wnt/β-catenin signal pathways. Conclusion: These findings suggest that suppression of H19 expression promotes H₂O₂-induced PC-12 cell injury, while downregulation of miR-155 and overexpression of FOXO1 protects PC-12 cells from H₂O₂-induced injury via activation of PI3K/AKT and Wnt/β-catenin signaling pathways.

Keywords: lncRNA, H19, spinal cord injury, miR-155, FOXO1, PI3K/AKT, Wnt/β-catenin

Introduction

Spinal cord injury (SCI) is a common neurological disorder, which influences the quality of life and triggers serious socio-economical and psychosocial consequences. SCI can be divided into primary and secondary mechanisms of injury. Primary SCI is caused by mechanical disruption of the spinal cord, resulting into hemorrhage, edema, axonal and neuronal necrosis, and demyelination, followed by cyst formation and infarction [1]. Secondary SCI is induced by multiple processes, including neuronal and glial apoptosis, inflammation, glial scar formation, local edema/ischemia, and oxidative stress [2, 3]. Treatment of SCI remains to be challenging due to multiple factors, such as axonal disruption, extensive cell loss, lack of

growth-promoting molecules, and excess of growth-inhibiting molecules in the scar [4]. Due to the devastating nature of SCI, prevention, treatment, and rehabilitation of SCI has become very essential. Understanding of secondary mechanisms will serve as a basis for the development of targeted pharmacological strategies to promote neuroprotection and restoration while alleviating ongoing neural injury.

It has been reported that non-coding RNAs have significant regulatory functions in SCI [5-7]. Noncoding RNAs can be divided into short non-coding RNAs (which include microRNA) and long non-coding RNAs (lncRNAs). lncRNAs are transcripts longer than 200 nucleotides, and can regulate gene expression at the level of chromatin modification, transcription and post-

transcriptional processing through different mechanisms [5]. Several studies have revealed that lncRNAs are abundant in the central nervous system (CNS) and are involved in several neurological conditions, including neurodevelopmental, neurodegenerative and neuroimmunological disorders; primary brain tumors; and psychiatric diseases [8, 9].

The H19 gene produces lncRNA that is 2.3 kb long [10]. lncRNA H19 is highly expressed in extraembryonic tissues, embryo proper and most fetal tissues, but the expression was significantly reduced after birth [11]. The functions of H19 reported by researchers are contradicting. Few studies reported that H19 is a tumor suppressor gene [10], while other studies showed that H19 was overexpressed in many malignancies, including breast cancer [12, 13], bladder cancer [14, 15], and cervical carcinoma [16]. Role of H19 in cell injury was evaluated in very few studies. Kim et al reported that H19 was re-expressed in rat vascular smooth muscle cells after injury [17]. However, role of H19 in SCI is still unclear and needs to be explored. In the present study, we evaluated the role of H19 in SCI by measuring its impact on hydrogen peroxide (H_2O_2)-injured pheochromocytoma (PC-12) cells, and exploring its underlying mechanisms.

Materials and methods

Cell culture and H_2O_2 treatment

PC-12 cells used in the study were purchased from Kunming Institute of Zoology (Kunming, China). The cells were seeded in flasks at a density of 1×10^4 cells/ml in Dulbecco's Modified Eagle's Medium (DMEM) with 10% (v/v) fetal bovine serum, 100 U/ml penicillin and 100 μ g/ml streptomycin. This mixture was maintained at 37°C in a humidified incubator containing 5% CO_2 . In hypoxia and normoxia culture conditions, the O_2 concentration was 3% and 21%, respectively. Culture medium was changed every other day. For H_2O_2 treatment, the cells were plated in cell culture multi-well plates (Thermo Scientific, Nunc™, Denmark) at a density of 5×10^4 cells/m for 24 h. The cells were treated with fresh medium with 200 μ M of H_2O_2 for 24 h to construct the injury model. The control group was treated with the same medium without H_2O_2 .

Quantitative reverse transcription polymerase chain reaction (qRT-PCR)

Total RNA was extracted from cells and tissues using Trizol reagent (Life Technologies Corporation, Carlsbad, CA, USA) according to the manufacturer's instructions. One Step SYBR® PrimeScript®PLUS RT-RNA PCR Kit (TaKaRa Biotechnology, Dalian, China) was used for the real-time PCR analysis to test the expression levels of H19. TaqMan MicroRNA Reverse Transcription Kit and Taqman Universal Master Mix II with the TaqMan MicroRNA Assay of miR-155 and U6 (Applied Biosystems, Foster City, CA, USA) were used for testing the expression levels of miR-155 in cells and tissues. For the test of forkhead box protein O1 (FOXO1), RNA PCR Kit (AMV) Version 3.0 (TaKaRa Biotechnology, Dalian, China) was used. Glyceraldehyde 3-phosphate dehydrogenase (GAPDH) used in this study for normalizing fold changes was calculated by relative quantification ($2^{-\Delta\Delta Ct}$) method.

Transfection and generation of stably transfected cell lines

Short-hairpin (sh)RNA directed against human lncRNA H19 was ligated into the U6/GFP/Neo plasmid (GenePharma, Shanghai, China) and was referred to as sh-H19. For the analysis of the FOXO1 functions, the full-length FOXO1 sequences and short-hairpin RNA directed against FOXO1 were constructed in pEX-2 and U6/GFP/Neo plasmids (GenePharma), respectively. They were referred to as pEX-FOXO1 and sh-FOXO1, respectively. Lipofectamine 3000 reagent (Life Technologies Corporation, Carlsbad, CA, USA) was used for cells transfection, according to the manufacturer's instructions. The plasmid carrying a non-targeting sequence was used as a negative control (NC) of sh-H19 and sh-FOXO1, and was referred to as sh-NC. The stably transfected cells were selected by the culture medium containing 0.5 mg/ml G418 (Sigma-Aldrich, St Louis, MO, USA). After approximately 4 weeks, G418-resistant cell clones were established. microRNA (miR)-155 mimics, inhibitors and their respective NC were synthesized (Life Technologies Corporation, MD, USA) and transfected into cells. Because the highest transfection efficiency occurred at 48 h, the 72 h time point post transfection was considered as the harvest time in the subsequent experiments.

Cell viability assay

For cell viability assay, 1×10^5 cells were seeded in duplicate in 60 mm dishes. At the indicated time periods, cells were washed and live cell numbers were determined by trypan blue exclusion.

Apoptosis assay

Cell apoptosis analysis was performed using propidium iodide (PI) and fluorescein isothiocyanate (FITC)-conjugated Annexin V staining. Briefly, cells were washed in phosphate buffered saline (PBS) and fixed in 70% ethanol. Fixed cells were then washed twice in PBS and stained in PI/FITC-Annexin V in the presence of 50 $\mu\text{g}/\text{ml}$ RNase A (Sigma-Aldrich), and then incubated for 1 h at room temperature in the dark. Flow cytometry analysis was done using a FAC Scan (Beckman Coulter, Fullerton, CA, USA). The data were analyzed using FlowJo software.

Migration and invasion assay

Cell migration was determined using a modified two-chamber migration assay with a pore size of 8 μm . For the migration assay, cells suspended in 200 μl of serum-free medium were seeded on the upper compartment of 24-well Transwell culture chamber, and 600 μl of complete medium was added to the lower compartment. After incubation at 37°C , cells were fixed with methanol. Non-traversed cells were removed from the upper surface of the filter carefully with a cotton swab. Traversed cells on the lower side of the filter were stained with crystal violet and counted.

Cell invasion was determined using 24-well Millicell Hanging Cell Culture inserts with 8 μm PET membranes (Millipore, Bedford, Massachusetts, USA). Briefly, after the cells were treated for indicated condition, 5.0×10^4 cells in 200 μl serum-free DMEM were plated in BD BioCoat™ Matrigel™ Invasion Chambers (8 μm pore size polycarbonate filters; BD Biosciences), while complete medium containing 10% fetal bovine serum was added to the lower chamber. After processing the invasion chambers for 48 hours (37°C , 5% CO_2) in accordance with the manufacturer's protocol, the non-invading cells were removed with a cotton swab; the invading cells were fixed in 100% methanol and then stained with crystal violet solution and counted micro-

scopically. The data are presented as the average number of cells attached to the bottom surface from five randomly chosen fields.

Reporter vectors construction and luciferase reporter assay

The fragment from H19 containing the predicted miR-155 binding site was amplified by PCR and then cloned into a pmirGLO Dual-luciferase miRNA Target Expression Vector (Promega, Madison, WI, USA) to form the reporter vector H19-wild-type (H19-Wt). To mutate the putative binding site of miR-155 in H19, the sequence of putative binding site was replaced and was named as H19-mutated-type (H19-Mt). Then the vectors and miR-155 mimics were co-transfected into PC-12 cells, and the Dual Luciferase Reporter Assay System (Promega, Madison, WI, USA) was used for testing luciferase activity.

Western blot analysis

The proteins used for western blotting were extracted using radioimmunoprecipitation assay (RIPA) lysis buffer (Beyotime Biotechnology, Shanghai, China) supplemented with protease inhibitors (Roche, Guangzhou, China). The proteins were quantified using the BCA™ Protein Assay Kit (Pierce, Appleton, WI, USA). The western blot system was established using a Bio-Rad Bis-Tris Gel system according to the manufacturer's instructions. Primary antibodies were prepared in 5% blocking buffer at a dilution of 1:1000. Primary antibody was incubated with the membrane at 4°C overnight, followed by wash and incubation with secondary antibody marked by horseradish peroxidase for 1 hour at room temperature. After rinsing, the polyvinylidene difluoride membrane carried blots and the antibodies were transferred into the Bio-Rad ChemiDoc™ XRS system, and then 200 μl Immobilon Western Chemiluminescent HRP Substrate (Millipore, MA, USA) was added to cover the membrane surface. The signals were captured and the intensity of the bands was quantified using Image Lab™ Software (Bio-Rad, Shanghai, China).

Statistical analysis

All experiments were repeated three times, and the results are presented as mean \pm SD. Statistical analyses were performed using GraphPad 6.0 statistical software. *P*-values were calculated using one-way analysis of vari-

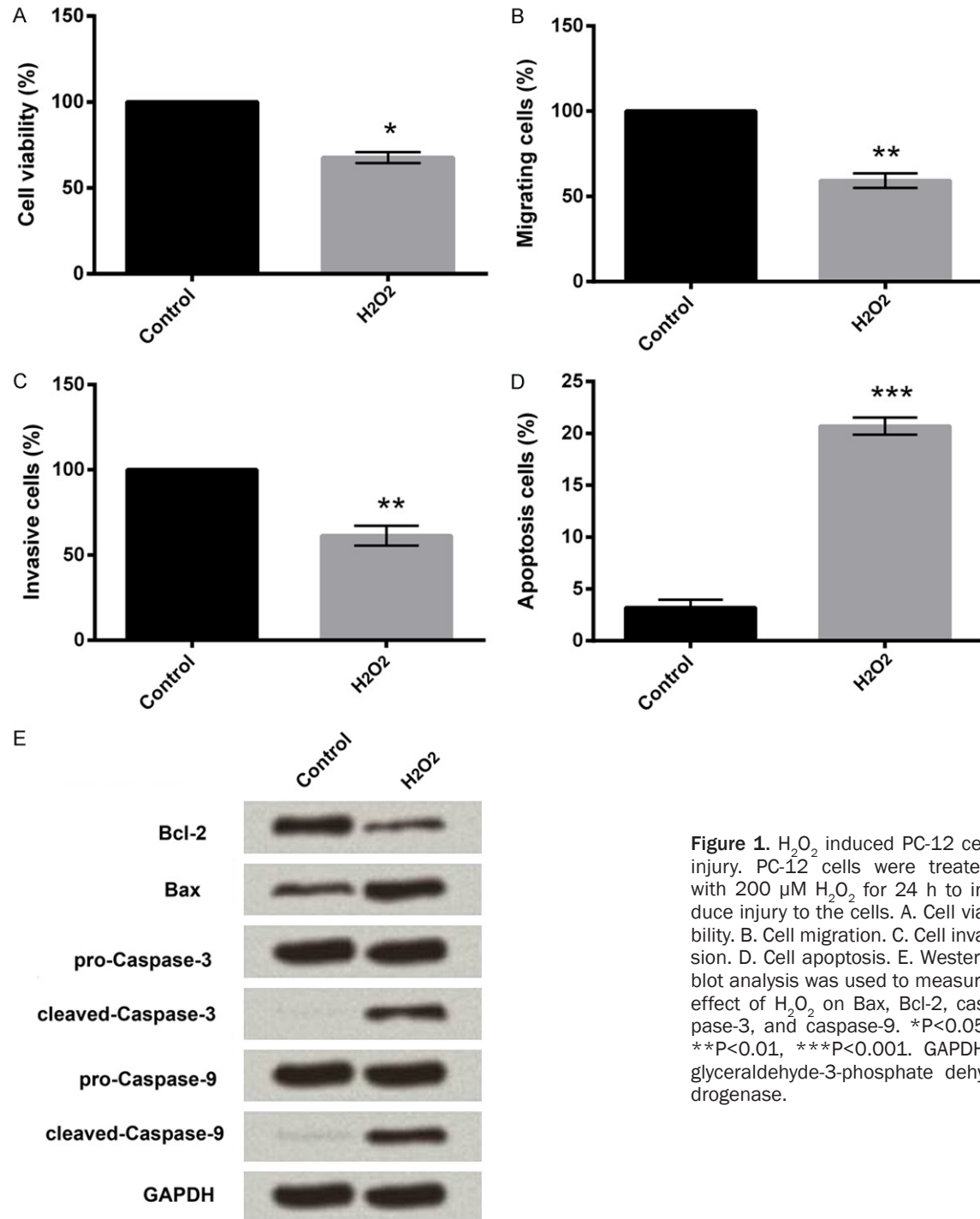


Figure 1. H₂O₂ induced PC-12 cell injury. PC-12 cells were treated with 200 μ M H₂O₂ for 24 h to induce injury to the cells. A. Cell viability. B. Cell migration. C. Cell invasion. D. Cell apoptosis. E. Western blot analysis was used to measure effect of H₂O₂ on Bax, Bcl-2, caspase-3, and caspase-9. *P<0.05, **P<0.01, ***P<0.001. GAPDH: glyceraldehyde-3-phosphate dehydrogenase.

ance. *P*-value of <0.05 was considered to indicate a statistically significant result.

Results

H₂O₂ induced PC-12 cell injury

We treated PC-12 cells with 200 μ M H₂O₂ for 24 h to induce injury in the cells. To confirm injury

to the cells, H₂O₂-treated cells and control cells (without H₂O₂ treatment) were subjected to different analyses, viz. cell viability, invasion, migration, and apoptosis. As compared to the control group, H₂O₂ significantly decreased cell viability (P<0.05; **Figure 1A**), migration (P<0.01; **Figure 1B**), and invasion (P<0.01; **Figure 1C**); but increased apoptosis (P<0.001; **Figure 1D**).

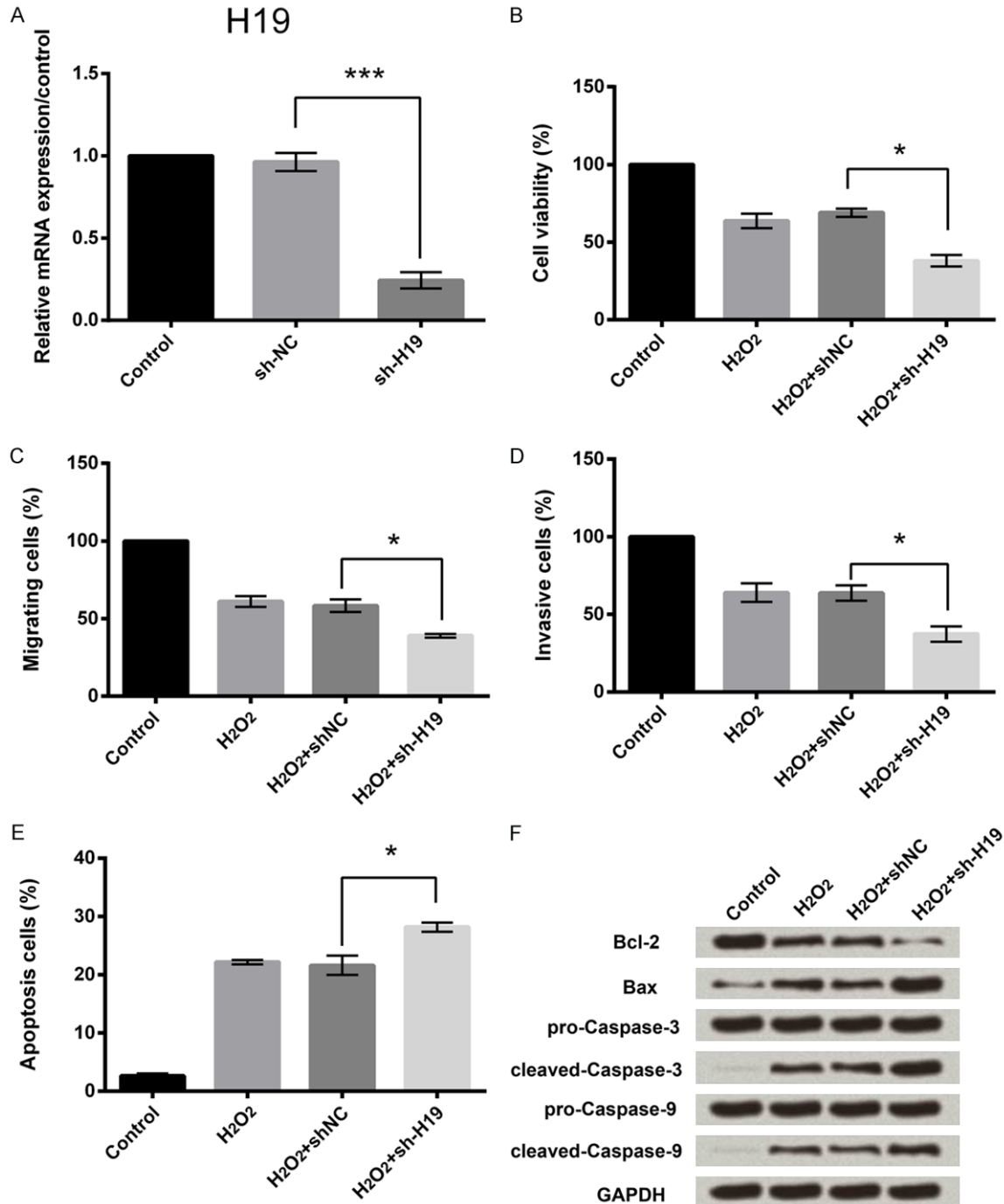


Figure 2. Suppression of H19 promoted H₂O₂-induced cell injury. A. Quantitative RT-PCR was used to measure relative mRNA expression of short-hairpin RNA-suppressed H19 (sh-H19), sh-NC, or control. B. Cell viability; C. migration; D. invasion, and E. apoptosis results of the injured PC-12 cells, transfected with control, H₂O₂, H₂O₂ + sh-NC, or H₂O₂ + sh-H19. E. Western blot analysis results for apoptosis. *P<0.05, ***P<0.001. GAPDH: glyceraldehyde-3-phosphate dehydrogenase; NC: negative control; RT-PCR: reverse transcription polymerase chain reaction.

Effect of H₂O₂ on cell apoptosis was also determined using western blot analysis. As shown in **Figure 1E**, H₂O₂ decreased the expression of anti-apoptotic protein (Bcl-2) and increased the

expression of pro-apoptotic proteins (Bax, caspase-3, and caspase-9). These findings together confirm that H₂O₂ induced injury in the PC-12 cells.

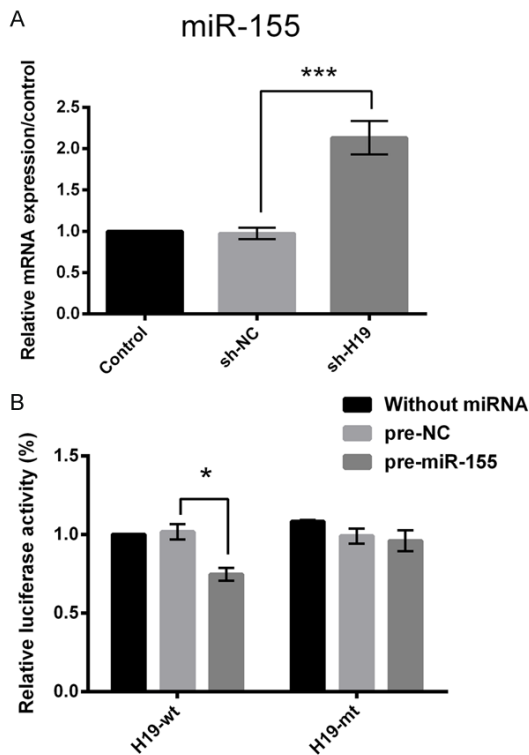


Figure 3. MiR-155 was a target of H19. A. Quantitative RT-PCR was used to measure relative mRNA expression of miR-155 in PC-12 cells transfected with short-hairpin RNA-suppressed H19 (sh-H19), sh-NC, or control. *** $P < 0.001$. B. Relative luciferase activity of H19-wild-type (H19-Wt) and H19-mutated-type (H19-Mt) vectors in PC-12 cells transfected with control (without miRNA), pre-NC, or pre-miR-155. * $P < 0.05$. NC: negative control; RT-PCR: reverse transcription polymerase chain reaction.

Suppression of H19 promoted H_2O_2 -induced cell injury

To measure the role of H19 in cell injury, we suppressed the expression of H19 in the cells using short-hairpin RNA, and then measured the cell viability, migration, invasion, and apoptosis of the injured cells. The cells were then transfected with H_2O_2 , H_2O_2 + sh-NC (short-hairpin RNA negative control), or H_2O_2 + sh-H19. **Figure 2A** showed that short-hairpin RNA significantly suppressed mRNA expression of H19 as compared to that of NC ($P < 0.005$). Further, suppression of H19 significantly decreased cell viability ($P < 0.05$; **Figure 2B**), migration ($P < 0.05$; **Figure 2C**), and invasion ($P < 0.05$; **Figure 2D**); and increased apoptosis ($P < 0.05$; **Figure 2E**) as compared with NC. The western blot results showed that the suppression of H19 decreased the expression of Bcl-2 and increased the

expression of Bax, caspase-3, and caspase-9 (**Figure 2F**). These findings indicated that suppression of H19 expression promoted H_2O_2 -induced cell injury.

MiR-155 was a target of H19

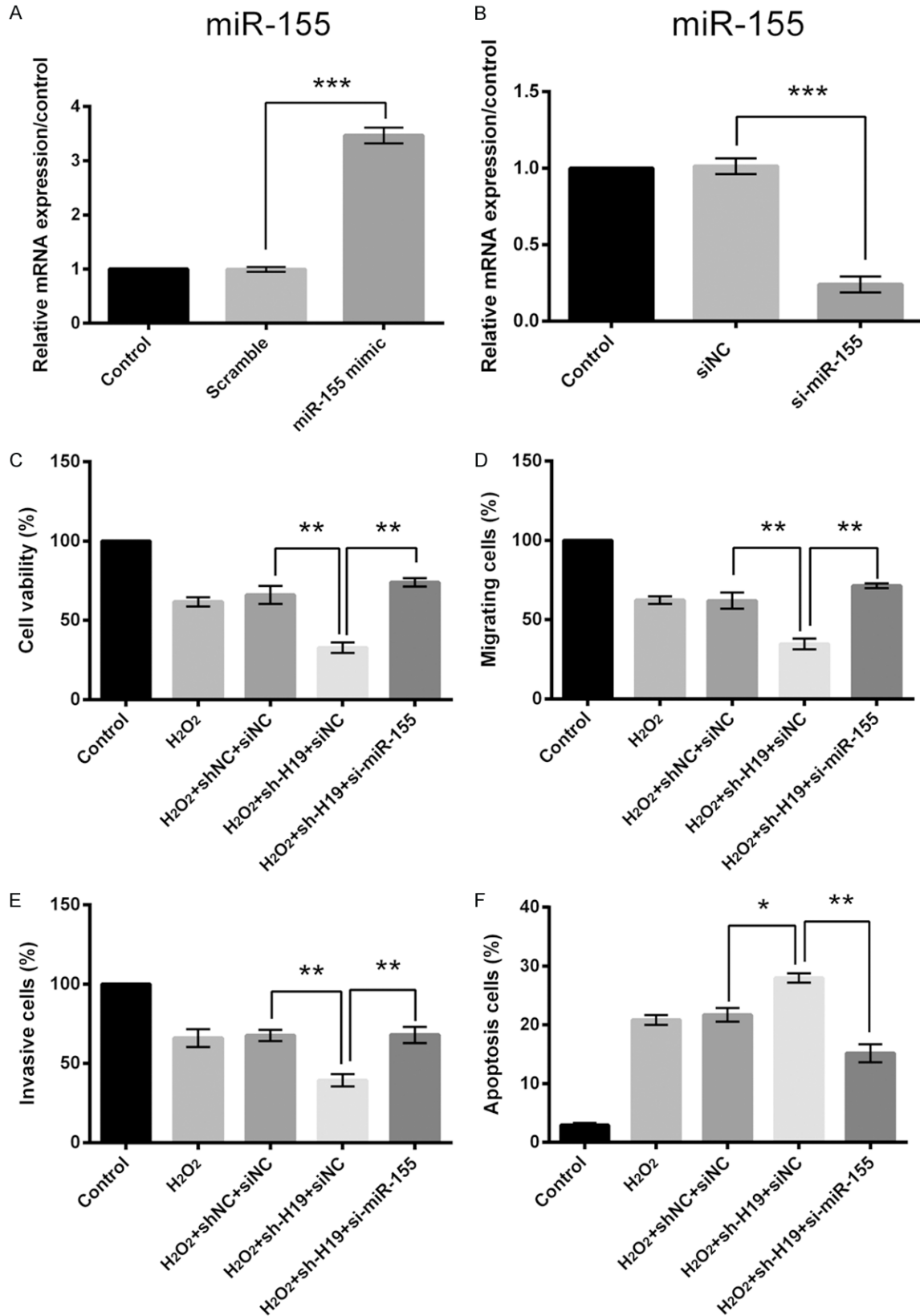
Although lncRNAs are functionally and structurally different from microRNAs, few studies have suggested a connection between these two classes of RNAs [11, 18]. Therefore, to identify a possible connection of H19 with microRNA, we measured the relative mRNA expression of miR-155 in PC-12 cells, with suppression of H19. **Figure 3A** showed that mRNA expression of miR-155 was significantly increased in the absence of H19 expression as compared with NC ($P < 0.005$), suggesting that H19 negatively regulated the expression of miR-155.

To further confirm that miR-155 is a target of H19, dual luciferase reporter assay was performed. For this assay, two types of vector were constructed: H19-wild-type (H19-Wt) and H19-mutated-type (H19-Mt). Then, the vectors and miR-155 mimics or NC were co-transfected into PC-12 cells, and luciferase activity was measured. As shown in **Figure 3B**, luciferase activity was significantly decreased in the cells co-transfected with miR-155 and H19-Wt as compared to the NC ($P < 0.05$), and no significant changes were observed with H19-Mt vector. These findings indicated that miR-155 was a target of H19.

Downregulation of miR-155 protected cells from H_2O_2 -induced injury

As miR-155 was identified as a target of H19, we studied the effect of miR-155 on H_2O_2 -induced cell injury, with suppressed expression of H19. We used miR-155 mimic to increase mRNA expression and si-miR-155 to decrease mRNA expression of miR-155 in the cells. As compared to the control group, miR-155 mimic significantly increased mRNA expression level of miR-155 ($P < 0.001$; **Figure 4A**), and si-miR-155 significantly decreased the expression ($P < 0.001$; **Figure 4B**).

After confirming the transfection efficiency of miR-155 mimic and inhibitor, we studied their effect on cell viability, migration, invasion, and apoptosis of the injured cells, with suppressed



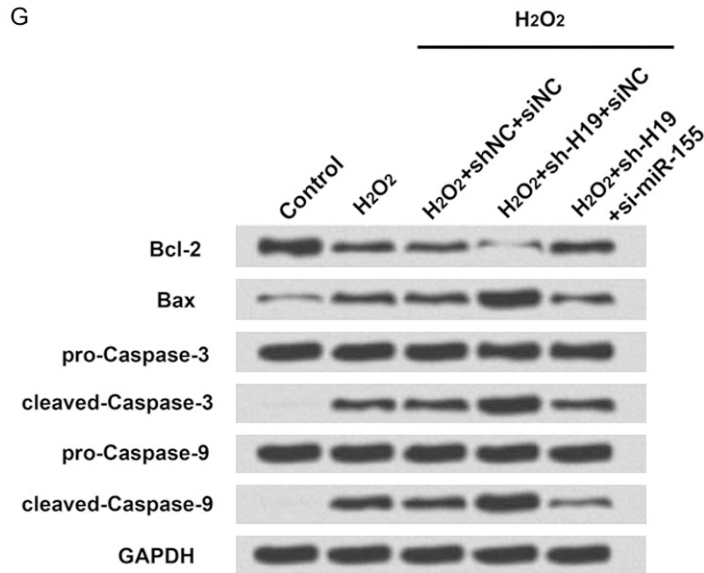


Figure 4. Downregulation of miR-155 protected PC-12 cells from H₂O₂-induced injury. Quantitative RT-PCR was used to measure relative mRNA expression of miR-155 in PC-12 cells transfected with control, scramble, or miR-155 mimic (A) or control, siNC, or si-miR-155 (B). (C) Cell viability; (D) migration; (E) invasion; and (F) apoptosis results of the injured PC-12 cells, transfected with control, H₂O₂, H₂O₂ + sh-NC + siNC, H₂O₂ + sh-H19 + siNC, or H₂O₂ + sh-H19 + si-miR-155. (G) Western blot analysis results for apoptosis. *P<0.05, **P<0.01, ***P<0.001. GAPDH: glyceraldehyde-3-phosphate dehydrogenase; NC: negative control; RT-PCR: reverse transcription polymerase chain reaction.

expression of H19. The results showed that downregulation of miR-155 significantly increased viability (P<0.01; **Figure 4C**), migration (P<0.01; **Figure 4D**), and invasion (P<0.01; **Figure 4E**); and decreased apoptosis (P<0.01; **Figure 4F**) of H₂O₂-injured PC12 cells. Western blot analysis results showed that the downregulation of miR-155 increased the expression of Bcl-2 and decreased the expression of Bax, caspase-3, and caspase-9 (**Figure 4G**). These findings indicated that downregulation of miR-155 expression protected PC-12 cells from H₂O₂-induced injury.

miR-155 downregulated FOXO1 expression

The forkhead box O (FOXO) transcription factors are essential for the regulation of stress response and ageing. FOXO1 belongs to the FOXO family [19]. As FOXO1 is involved in stress response, we measured the effect of miR-155 on the expression level of FOXO1. The results showed that, as compared to the control group, miR-155 mimic significantly decreased the mRNA expression level of FOXO1 (P<0.01; **Figure 5A, 5C**), while si-miR-155 increased FOXO1 expression (P<0.001; **Figure 5B, 5C**). These results indicated that miR-155 negatively regulated FOXO1 expression.

To confirm that FOXO1 is a target of miR-155, dual luciferase reporter assay was performed. The vectors (FOXO1-Wt and FOXO1-Mt) and miR-155 mimics or NC were co-transfected into PC-12 cells. As shown in **Figure 5D**, luciferase

activity significantly decreased in cells co-transfected with miR-155 and FOXO1-Wt, as compared to the NC (P<0.05); no significant changes were observed with FOXO1-Mt vector. These findings suggest that FOXO1 was a target of miR-155.

Overexpression of FOXO1 decreased H₂O₂-induced cell injury

For analyzing the functions of FOXO1, full-length FOXO1 sequences and short-hairpin RNA directed against FOXO1 were constructed in pEX-2 and U6/GFP/Neo plasmids and were referred to as pEX-FOXO1 and sh-FOXO1, respectively. The qRT-PCR and western blot results showed that pEX-FOXO1 significantly increased the mRNA expression of FOXO1 (P<0.001; **Figure 6A and 6C**), while sh-FOXO1 decreased the expression (P<0.001; **Figure 6B and 6C**), respectively, as compared to that of the control group.

In further experiments, we used pEX-FOXO1 and sh-FOXO1 to measure the effect of FOXO1 on cell viability, migration, invasion, and apoptosis of the injured cells. The results showed that pEX-FOXO1 significantly increased cell viability (P<0.05; **Figure 6D**), migration (P<0.05; **Figure 6E**), and invasion (P<0.05; **Figure 6F**); and decreased apoptosis (P<0.01; **Figure 6G**) as compared with cells treated with H₂O₂ and pEX. Conversely, sh-FOXO1 significantly decreased cell viability (P<0.01; **Figure 6D**), migration (P<0.01; **Figure 6E**), and invasion (P<0.05;

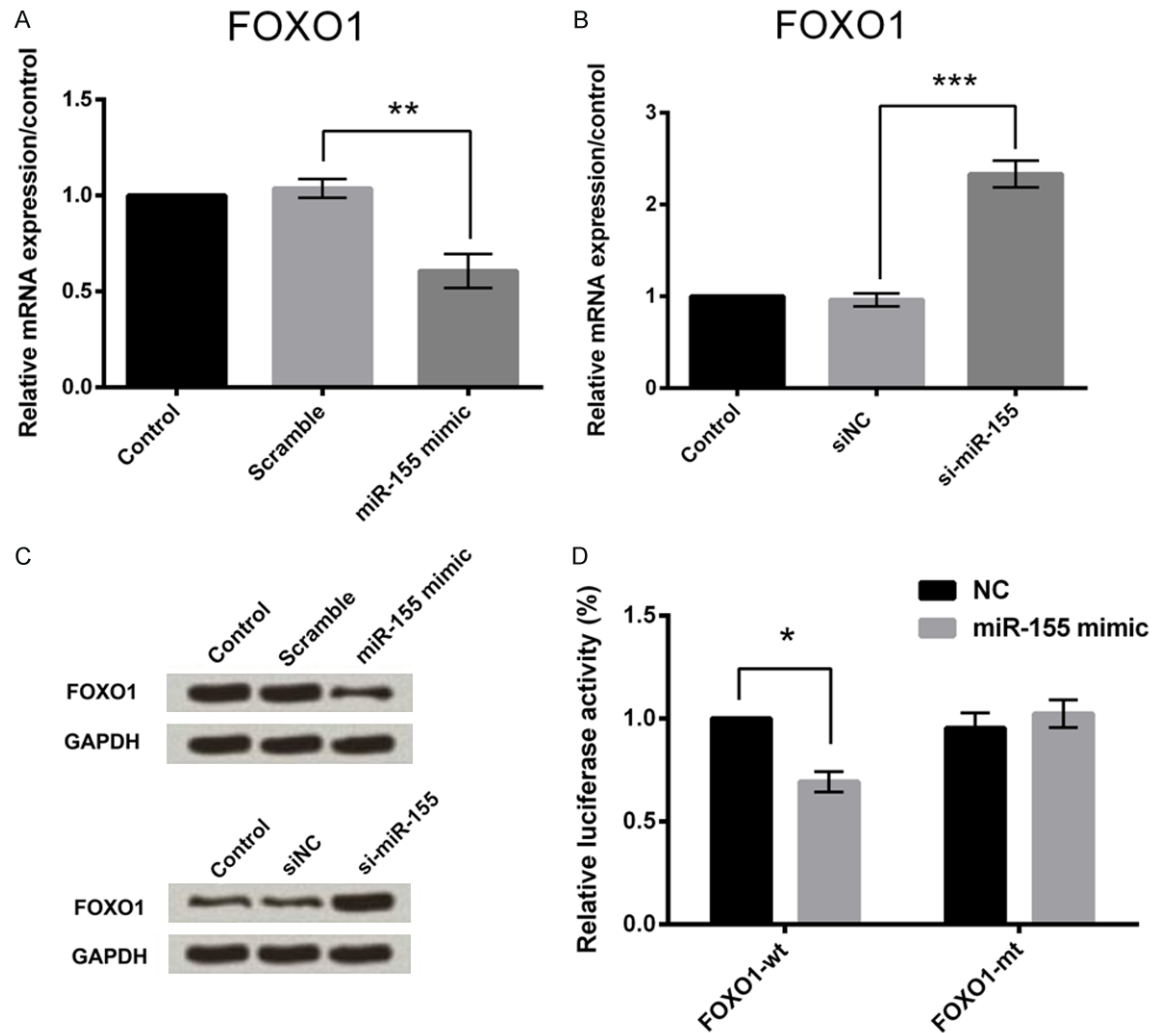


Figure 5. MiR-155 downregulated FOXO1 expression. Quantitative RT-PCR was used to measure relative mRNA expression of FOXO1 in PC-12 cells transfected with control, scramble, or miR-155 mimic (A) or control, siNC, or si-miR-155 (B). (C) Western blot analysis results of (A) and (B). (D) Relative luciferase activity of FOXO1-wild-type (FOXO1-Wt) and FOXO1-mutated-type (FOXO1-Mt) vectors in PC-12 cells transfected with NC or miR-155 mimic. * $P < 0.05$, ** $P < 0.01$, *** $P < 0.001$. GAPDH: glyceraldehyde-3-phosphate dehydrogenase; NC: negative control; RT-PCR: reverse transcription polymerase chain reaction.

Figure 6F); and increased apoptosis ($P < 0.01$; **Figure 6G**) as compared with the cells treated with H_2O_2 and shNC. Western blot results showed that the overexpression of FOXO1 increased the expression of Bcl-2 and decreased the expression of Bax, caspase-3, and caspase-9, while suppression of FOXO1 expression reversed these results (**Figure 6H**). These findings suggested that overexpression of FOXO1 decreased H_2O_2 -induced PC-12 cell injury.

FOXO1 activates PI3K/AKT and Wnt/ β -catenin signal pathways

We then studied the underlying mechanism for these effects by measuring the effect of

FOXO1 on PI3K/AKT and Wnt/ β -catenin pathways using western blot analysis. The results showed that overexpression of FOXO1 increased the expression of phosphorylated PI3K and AKT, Wnt3a, Wnt5a, and β -catenin, while suppression of FOXO1 reversed these results (**Figure 7**). These findings indicated that FOXO1 decreased H_2O_2 -induced cell injury by activating PI3K/AKT and Wnt/ β -catenin signal pathways.

Discussion

In the present study, we evaluated the effects and mechanisms of lncRNA H19 on H_2O_2 -induced PC-12 cell injury. In the first step, H_2O_2

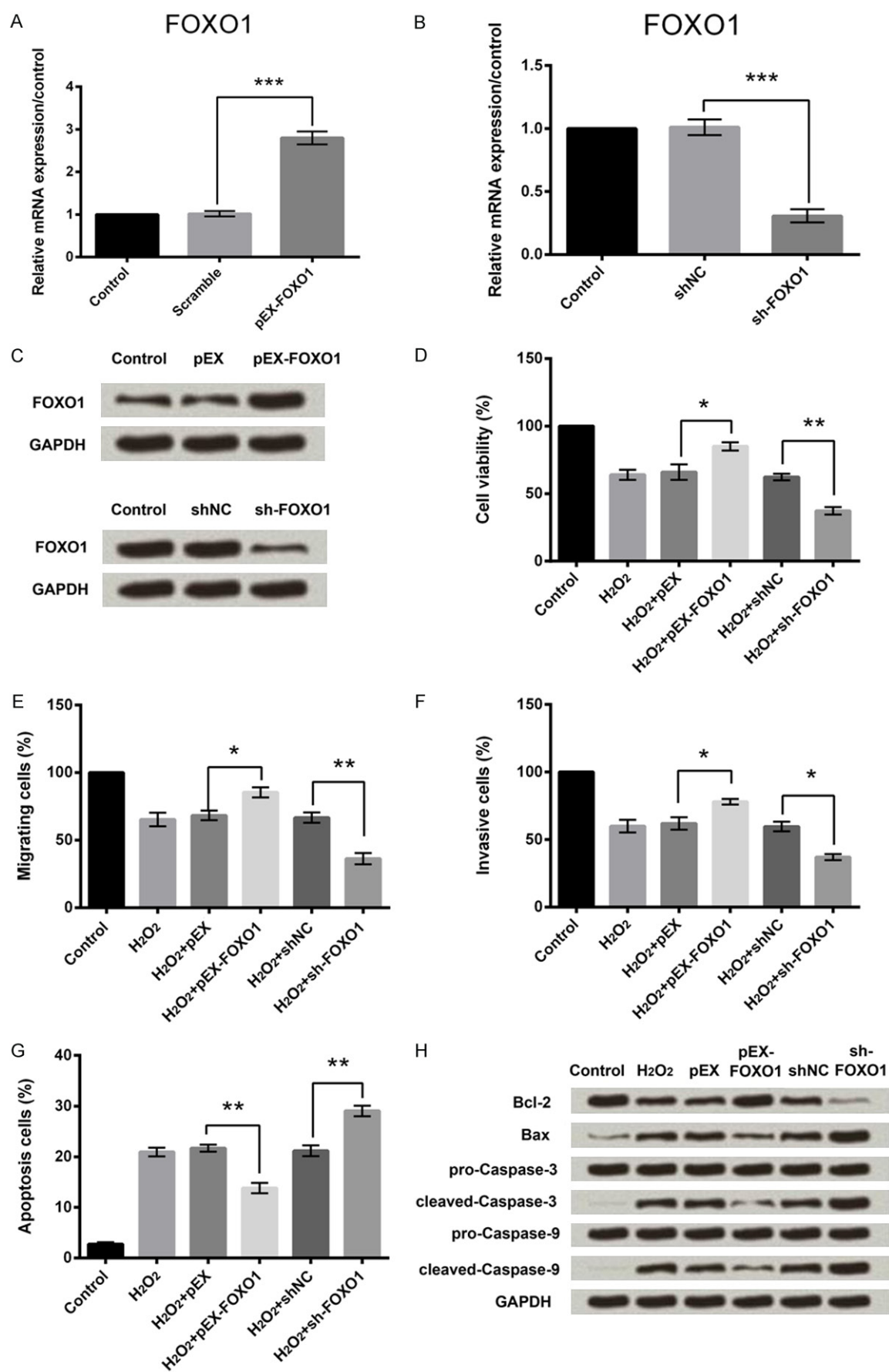


Figure 6. Overexpression of FOXO1 decreased H_2O_2 -induced cell injury. Quantitative RT-PCR was used to measure relative mRNA expression of FOXO1 in PC-12 cells transfected with control, scramble, or pEX-FOXO1 (A) or control, siNC, or sh-FOXO1 (B). (C) Western blot analysis results of (A) and (B). (D) Cell viability; (E) migration; (F) invasion; and (G) apoptosis results of the injured PC-12 cells, transfected with control, H_2O_2 , H_2O_2 + pEX, H_2O_2 + pEX-FOXO1, H_2O_2 + shNC, or H_2O_2 + sh-FOXO1. (H) Western blot analysis results for apoptosis. * $P < 0.05$, ** $P < 0.01$, *** $P < 0.001$. GAPDH: glyceraldehyde-3-phosphate dehydrogenase; NC: negative control; FOXO1, forkhead box protein O1; RT-PCR: reverse transcription polymerase chain reaction.

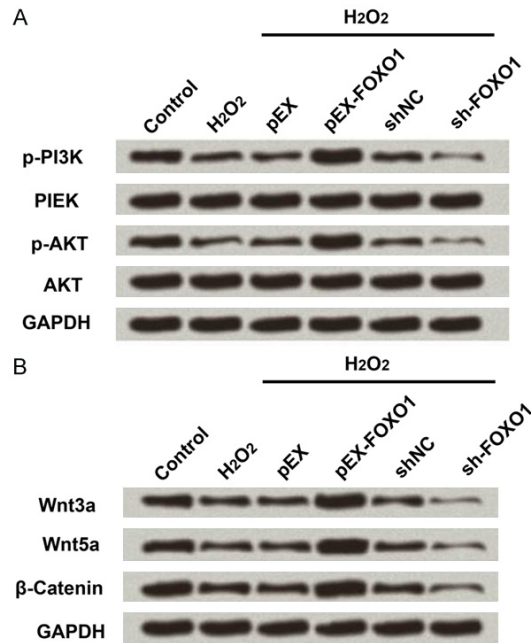


Figure 7. FOXO1 activates PI3K/AKT pathway. Western blot analysis was used to measure expressions of PI3K, phosphorylated PI3K, AKT, phosphorylated AKT, AKT, Wnt3a, Wnt5a, and β -catenin in PC-12 cells transfected with control, H_2O_2 , pEX, pEX-FOXO1, shNC, or sh-FOXO1. AKT: serine-threonine kinase; GAPDH: glyceraldehyde-3-phosphate dehydrogenase; NC: negative control; FOXO1, forkhead box protein O1; PI3K: phosphoinositide 3-kinase.

induced injury to PC-12 cells by decreasing its viability, migration, and invasion and increasing apoptosis. Subsequently, we suppressed the expression of H19 and found that this suppression further promoted H_2O_2 -induced cell injury. Further experiments found miR-155 as a potential target of H19 as the expression of miR-155 was negatively regulated by H19. Interestingly, downregulation of miR-155 protected PC-12 cells from H_2O_2 -induced injury. Then, we studied the underlying mechanisms and found that FOXO1 was negatively regulated by miR-155. Overexpression of FOXO1 decreased H_2O_2 -induced cell injury by activating PI3K/AKT and Wnt/ β -catenin signaling pathways.

H_2O_2 is a reactive oxygen species (ROS) which possesses higher reactivity than molecular oxy-

gen. During oxidative stress, ROS is produced in excess quantity which results in growth arrest, senescence, and death of the cells. Oxidative stress has been implicated in a variety of diseases, including SCI [20]. It has been reported that infiltrating neutrophils release ROS at the site of SCI; therefore, ROS plays a key role in the secondary damage of SCI [21]. Thus, we chose H_2O_2 to induce injury to PC-12 cells and built an oxidative stress model. PC-12 is a rat cell line derived from a pheochromocytoma of the adrenal medulla [22]. PC-12 cells show unique sensitivity to changes in oxygen availability and have been used in many in vitro studies of SCI [23, 24].

We demonstrated that H_2O_2 decreased viability, migration and invasion and increased apoptosis of PC-12 cells. We further conducted a western blot test to measure effect of H_2O_2 on the expression of anti-apoptotic protein (Bcl-2) and pro-apoptotic proteins (Bax, caspase-3, and caspase-9). Previous studies reported that the Bcl-2 family and the caspase family play crucial roles in H_2O_2 -induced apoptosis in PC-12 cells [25, 26]. Caspase-3 is synthesized as an inactive precursor (pro-caspase-3), which is cleaved proteolytically to produce a mature enzyme (cleaved-caspase-3); cleaved-caspase-9 is produced the same way [27]. Our results showed that H_2O_2 decreased the expression of Bcl-2 and increased the expression of Bax, cleaved-caspase-3, and cleaved-caspase-9. Other studies have reported similar results. These reports showed that H_2O_2 downregulated Bcl-2 expression and increased caspase-3 expression [25, 26].

Role of lncRNA H19 has been studied in many malignant diseases. Majority of the studies have demonstrated that H19 increases cell viability and decreases apoptosis. Ma et al reported that H19 promoted cell proliferation in pancreatic ductal adenocarcinoma [28]. Likewise, Yang et al demonstrated that upregulation of H19 increased cell proliferation and downregulation increased apoptosis of gastric cancer cells [29]. In our study, we demonstrat-

ed that downregulation of H19 decreased cell viability, migration, and invasion and increased apoptosis of H₂O₂-injured PC-12 cells. To our knowledge, this is the first study to report the effects of H19 on H₂O₂-injured PC-12 cells.

MicroRNAs are small, non-coding RNAs that regulate the expression of protein-encoding genes at the post-transcriptional level. MicroRNAs are involved in various cellular processes such as cell proliferation, apoptosis, and differentiation [6, 30, 31]. It has been reported that microRNAs play key role in the process of nerve development and injury repair [6, 32, 33]. In our study, we identified miR-155 as a potential target of H19. It has been suggested that miR-155 was involved in many biological processes, including inflammation and immunity [34]. MiR-155 was upregulated during SCI, which causes inflammatory destruction of the spinal cord [35]. Yi et al reported that miR-155 deficiency suppresses Th17 cell differentiation and improves locomotor recovery after SCI [36]. Another report suggested that suppression of miR-155 decreases neuropathic pain [37]. In consistence with these reports, we demonstrated that downregulation of miR-155 protected PC-12 cells from H₂O₂-induced injury by increasing cell viability, migration, and invasion and decreasing apoptosis.

Luciferase reporter assay identified FOXO1 as a target of miR-155. In addition, miR-155 negatively regulated FOXO1 expression. In skeletal muscle of chronic SCI patients, decreased expression of FOXO1 mRNA and protein was noted [38]. In contrast, Long et al reported marked increase in the FOXO1 protein content and mRNA expression in skeletal muscle of SCI patients [39]. The reason for these different results is still not clear. In our study, overexpression of FOXO1 decreased H₂O₂-induced PC-12 cell injury by increasing cell viability, migration, and invasion and decreasing apoptosis. We explored the underlying mechanism using western blot analysis and found that FOXO1 exerts these effects by activating PI3K/AKT and Wnt/ β -catenin signal pathways. PI3K/AKT signal pathway is an important pathway for cell survival, proliferation, and migration [40]. Recent studies have shown that the activation of PI3K/AKT is crucial in protecting nerve cells against ischemia and anoxia neuron damage [41-44]. Wnt signaling pathway regulates cell

migration, cell fate determination, cell polarity, neural patterning and organogenesis during embryonic development [45]. It has been reported that Wnt proteins play crucial roles during CNS development and have been involved in several neurological diseases, including SCI [46].

In conclusion, this study demonstrated that suppression of lncRNA H19 promoted H₂O₂-induced injury to PC-12 cells by decreasing cell viability, migration, and invasion and increasing apoptosis. In addition, downregulation of miR-155, which was identified as a target of H19, protected PC-12 cells from H₂O₂-induced injury. FOXO1 was identified as a target of miR-155 and overexpression of FOXO1 protected PC-12 cells from H₂O₂-induced injury by activating PI3K/AKT and Wnt/ β -catenin signaling pathways. Our research might provide new insights in the prevention and treatment of SCI.

Disclosure of conflict of interest

None.

Address correspondence to: Yingmei Qi, Department of Orthopaedics, China-Japan Union Hospital of Jilin University, 126, Xiantai Street, Changchun 130033, P. R. China. E-mail: qiyingmei101@126.com

References

- [1] Dumont RJ, Okonkwo DO, Verma S, Hurlbert RJ, Boulos PT, Ellegala DB and Dumont AS. Acute spinal cord injury, part I: pathophysiologic mechanisms. *Clin Neuropharmacol* 2001; 24: 254-264.
- [2] Donnelly DJ and Popovich PG. Inflammation and its role in neuroprotection, axonal regeneration and functional recovery after spinal cord injury. *Exp Neurol* 2008; 209: 378-388.
- [3] Bareyre FM. Neuronal repair and replacement in spinal cord injury. *J Neurol Sci* 2008; 265: 63-72.
- [4] Estrada V and Muller HW. Spinal cord injury - there is not just one way of treating it. *F1000Prime Rep* 2014; 6: 84.
- [5] Mercer TR, Dinger ME and Mattick JS. Long non-coding RNAs: insights into functions. *Nat Rev Genet* 2009; 10: 155-159.
- [6] Bhalala OG, Srikanth M and Kessler JA. The emerging roles of microRNAs in CNS injuries. *Nat Rev Neurol* 2013; 9: 328-339.
- [7] Kapranov P, Cheng J, Dike S, Nix DA, Duttagupta R, Willingham AT, Stadler PF, Hertel J, Hackermuller J, Hofacker IL, Bell I, Cheung E, Dren-

- kow J, Dumais E, Patel S, Helt G, Ganesh M, Ghosh S, Piccolboni A, Sementchenko V, Tammana H and Gingeras TR. RNA maps reveal new RNA classes and a possible function for pervasive transcription. *Science* 2007; 316: 1484-1488.
- [8] Huarte M, Guttman M, Feldser D, Garber M, Koziol MJ, Kenzelmann-Broz D, Khalil AM, Zuk O, Amit I, Rabani M, Attardi LD, Regev A, Lander ES, Jacks T and Rinn JL. A large intergenic noncoding RNA induced by p53 mediates global gene repression in the p53 response. *Cell* 2010; 142: 409-419.
- [9] Qureshi IA, Mattick JS and Mehler MF. Long non-coding RNAs in nervous system function and disease. *Brain Res* 2010; 1338: 20-35.
- [10] Gabory A, Ripoche MA, Yoshimizu T and Dandolo L. The H19 gene: regulation and function of a non-coding RNA. *Cytogenet Genome Res* 2006; 113: 188-193.
- [11] Li H, Yu B, Li J, Su L, Yan M, Zhu Z and Liu B. Overexpression of lncRNA H19 enhances carcinogenesis and metastasis of gastric cancer. *Oncotarget* 2014; 5: 2318-2329.
- [12] Berteaux N, Lottin S, Monte D, Pinte S, Quatanens B, Coll J, Hondermarck H, Curgy JJ, Dugimont T and Adriaenssens E. H19 mRNA-like noncoding RNA promotes breast cancer cell proliferation through positive control by E2F1. *J Biol Chem* 2005; 280: 29625-29636.
- [13] Berteaux N, Aptel N, Cathala G, Genton C, Coll J, Daccache A, Spruyt N, Hondermarck H, Dugimont T, Curgy JJ, Forne T and Adriaenssens E. A novel H19 antisense RNA overexpressed in breast cancer contributes to paternal IGF2 expression. *Mol Cell Biol* 2008; 28: 6731-6745.
- [14] Luo M, Li Z, Wang W, Zeng Y, Liu Z and Qiu J. Upregulated H19 contributes to bladder cancer cell proliferation by regulating ID2 expression. *FEBS J* 2013; 280: 1709-1716.
- [15] Byun HM, Wong HL, Birnstein EA, Wolff EM, Liang G and Yang AS. Examination of IGF2 and H19 loss of imprinting in bladder cancer. *Cancer Res* 2007; 67: 10753-10758.
- [16] Kim SJ, Park SE, Lee C, Lee SY, Jo JH, Kim JM and Oh YK. Alterations in promoter usage and expression levels of insulin-like growth factor-II and H19 genes in cervical carcinoma exhibiting biallelic expression of IGF-II. *Biochim Biophys Acta* 2002; 1586: 307-315.
- [17] Kim DK, Zhang L, Dzau VJ and Pratt RE. H19, a developmentally regulated gene, is reexpressed in rat vascular smooth muscle cells after injury. *J Clin Invest* 1994; 93: 355-360.
- [18] Shi Y, Wang Y, Luan W, Wang P, Tao T, Zhang J, Qian J, Liu N and You Y. Long non-coding RNA H19 promotes glioma cell invasion by deriving miR-675. *PLoS One* 2014; 9: e86295.
- [19] Zhang X, Yalcin S, Lee DF, Yeh TY, Lee SM, Su J, Mungamuri SK, Rimmele P, Kennedy M, Sellers R, Landthaler M, Tuschl T, Chi NW, Lemischka I, Keller G and Ghaffari S. FOXO1 is an essential regulator of pluripotency in human embryonic stem cells. *Nat Cell Biol* 2011; 13: 1092-1099.
- [20] Yuan W, Guo J, Li X, Zou Z, Chen G, Sun J, Wang T and Lu D. Hydrogen peroxide induces the activation of the phospholipase C-gamma1 survival pathway in PC12 cells: protective role in apoptosis. *Acta Biochim Biophys Sin (Shanghai)* 2009; 41: 625-630.
- [21] Genovese T and Cuzzocrea S. Role of free radicals and poly(ADP-ribose)polymerase-1 in the development of spinal cord injury: new potential therapeutic targets. *Curr Med Chem* 2008; 15: 477-487.
- [22] Greene LA and Tischler AS. Establishment of a noradrenergic clonal line of rat adrenal pheochromocytoma cells which respond to nerve growth factor. *Proc Natl Acad Sci U S A* 1976; 73: 2424-2428.
- [23] Zompa EA, Pizzo DP and Hulsebosch CE. Migration and differentiation of PC12 cells transplanted into the rat spinal cord. *Int J Dev Neurosci* 1993; 11: 535-544.
- [24] Zhang H, Wu F, Kong X, Yang J, Chen H, Deng L, Cheng Y, Ye L, Zhu S, Zhang X, Wang Z, Shi H, Fu X, Li X, Xu H, Lin L and Xiao J. Nerve growth factor improves functional recovery by inhibiting endoplasmic reticulum stress-induced neuronal apoptosis in rats with spinal cord injury. *J Transl Med* 2014; 12: 130.
- [25] Liu CS, Chen NH and Zhang JT. Protection of PC12 cells from hydrogen peroxide-induced cytotoxicity by salvianolic acid B, a new compound isolated from *Radix Salviae miltiorrhizae*. *Phytomedicine* 2007; 14: 492-497.
- [26] Cho ES, Lee KW and Lee HJ. Cocoa procyanidins protect PC12 cells from hydrogen-peroxide-induced apoptosis by inhibiting activation of p38 MAPK and JNK. *Mutat Res* 2008; 640: 123-130.
- [27] Nicholson DW, Ali A, Thornberry NA, Vaillancourt JP, Ding CK, Gallant M, Gareau Y, Griffin PR, Labelle M, Lazebnik YA and et al. Identification and inhibition of the ICE/CED-3 protease necessary for mammalian apoptosis. *Nature* 1995; 376: 37-43.
- [28] Ma L, Tian X, Wang F, Zhang Z, Du C, Xie X, Kornmann M and Yang Y. The long noncoding RNA H19 promotes cell proliferation via E2F-1 in pancreatic ductal adenocarcinoma. *Cancer Biol Ther* 2016; 17: 1051-1061.
- [29] Yang F, Bi J, Xue X, Zheng L, Zhi K, Hua J and Fang G. Up-regulated long non-coding RNA H19 contributes to proliferation of gastric cancer cells. *FEBS J* 2012; 279: 3159-3165.

- [30] Slezak-Prochazka I, Durmus S, Kroesen BJ and van den Berg A. MicroRNAs, macrocontrol: regulation of miRNA processing. *RNA* 2010; 16: 1087-1095.
- [31] Bartel DP. MicroRNAs: genomics, biogenesis, mechanism, and function. *Cell* 2004; 116: 281-297.
- [32] Hutchison ER, Okun E and Mattson MP. The therapeutic potential of microRNAs in nervous system damage, degeneration, and repair. *Neuromolecular Med* 2009; 11: 153-161.
- [33] Wu D and Murashov AK. Molecular mechanisms of peripheral nerve regeneration: emerging roles of microRNAs. *Front Physiol* 2013; 4: 55.
- [34] Faraoni I, Antonetti FR, Cardone J and Bonmassar E. miR-155 gene: a typical multifunctional microRNA. *Biochim Biophys Acta* 2009; 1792: 497-505.
- [35] Martirosyan NL, Carotenuto A, Patel AA, Kalani MY, Yagmurlu K, Lemole GM Jr, Preul MC and Theodore N. The role of microrna markers in the diagnosis, treatment, and outcome prediction of spinal cord injury. *Front Surg* 2016; 3: 56.
- [36] Yi J, Wang D, Niu X, Hu J, Zhou Y and Li Z. MicroRNA-155 deficiency suppresses Th17 cell differentiation and improves locomotor recovery after spinal cord injury. *Scand J Immunol* 2015; 81: 284-290.
- [37] Tan Y, Yang J, Xiang K, Tan Q and Guo Q. Suppression of microRNA-155 attenuates neuropathic pain by regulating SOCS1 signalling pathway. *Neurochem Res* 2015; 40: 550-560.
- [38] Leger B, Senese R, Al-Khodairy AW, Deriaz O, Gobelet C, Giacobino JP and Russell AP. Atrogin-1, MuRF1, and FoXO, as well as phosphorylated GSK-3beta and 4E-BP1 are reduced in skeletal muscle of chronic spinal cord-injured patients. *Muscle Nerve* 2009; 40: 69-78.
- [39] Long YC, Kostovski E, Boon H, Hjeltne N, Krook A and Widegren U. Differential expression of metabolic genes essential for glucose and lipid metabolism in skeletal muscle from spinal cord injured subjects. *J Appl Physiol* (1985) 2011; 110: 1204-1210.
- [40] Chen CH, Sung CS, Huang SY, Feng CW, Hung HC, Yang SN, Chen NF, Tai MH, Wen ZH and Chen WF. The role of the PI3K/Akt/mTOR pathway in glial scar formation following spinal cord injury. *Exp Neurol* 2016; 278: 27-41.
- [41] Renfu Q, Rongliang C, Mengxuan D, Liang Z, Jinwei X, Zongbao Y and Disheng Y. Anti-apoptotic signal transduction mechanism of electroacupuncture in acute spinal cord injury. *Acupunct Med* 2014; 32: 463-471.
- [42] Qin DX, Zou XL, Luo W, Zhang W, Zhang HT, Li XL, Zhang H, Wang XY and Wang TH. Expression of some neurotrophins in the spinal motoneurons after cord hemisection in adult rats. *Neurosci Lett* 2006; 410: 222-227.
- [43] Kamei N, Tanaka N, Oishi Y, Hamasaki T, Nakanishi K, Sakai N and Ochi M. BDNF, NT-3, and NGF released from transplanted neural progenitor cells promote corticospinal axon growth in organotypic cocultures. *Spine (Phila Pa 1976)* 2007; 32: 1272-1278.
- [44] Guo JS, Zeng YS, Li HB, Huang WL, Liu RY, Li XB, Ding Y, Wu LZ and Cai DZ. Cotransplant of neural stem cells and NT-3 gene modified Schwann cells promote the recovery of transected spinal cord injury. *Spinal Cord* 2007; 45: 15-24.
- [45] Komiya Y and Habas R. Wnt signal transduction pathways. *Organogenesis* 2008; 4: 68-75.
- [46] Gonzalez-Fernandez C, Fernandez-Martos CM, Shields SD, Arenas E and Javier Rodriguez F. Wnts are expressed in the spinal cord of adult mice and are differentially induced after injury. *J Neurotrauma* 2014; 31: 565-581.